Desalination and Water Treatment
www.deswater.com

doi: 10.5004/dwt.2020.26004

197 (2020) 379–391
September

Chemical modification of pomelo leaves as a simple and effective way to enhance adsorption toward methyl violet dye

YieChen Lu[a], Linda B.L. Lim[a,*], N. Priyantha[b,c]

[a]*Chemical Sciences Program, Faculty of Science, Universiti Brunei Darussalam, Negara Brunei Darussalam, Tel. +00-673-8748010; emails: linda.lim@ubd.edu.bn (L.B.L. Lim), yiechen_93@hotmail.com (Y.C. Lu)*
[b]*Department of Chemistry, Faculty of Science, University of Peradeniya, Peradeniya, Sri Lanka*
[c]*Postgraduate Institute of Science, University of Peradeniya, Peradeniya, Sri Lanka, email: namal.priyantha@yahoo.com (N. Priyantha)*

Received 4 December 2019; Accepted 18 April 2020

ABSTRACT

The present research reports chemical modification using 1.0 M NaOH as an economical, simple, and yet effective way of enhancing the adsorption capacity of pomelo leaves (PL). The NaOH-PL was then tested for its adsorption toward methyl violet 2B (MV) dye. Fast equilibrium of the adsorbate–adsorbent system was achieved within 30 min. Further, the modified adsorbent also adsorbed well under varying environment conditions. Fitting of the kinetics and isotherm data were carried out using both the linear and nonlinear regression analyses and comparisons were made between the two methods. The adsorption obeyed the pseudo-second-order kinetics with rate constant (k_2) of 5.679 g mmol^{-1} min^{-1}. Regeneration studies showed that NaOH-PL displayed the ability to be regenerated and reused multiple times, even without treatment. However, when treated with either acid or base, its adsorption capacity was retained even at the fifth consecutive cycle of regeneration. The Sips model fitted well to the experimental adsorption isotherm based on linearized analyses, with maximum adsorption capacity (q_{max}) of 1,970 mg g^{-1}, a remarkably high value that surpasses those of many reported adsorbents. Nonlinear regression pointed toward the Redlich–Peterson and Langmuir models with q_{max} of 910.8 mg g^{-1} based on the latter model. Thus, the above findings indicate that NaOH-PL could find its application as a promising and an economical material in wastewater treatment given that its preparation from PL is a simple one-step method.

Keywords: Chemical modification; Pomelo leaf adsorbent; Methyl violet 2B dye; Adsorption isotherm; Regeneration; Kinetics

1. Introduction

Nowadays the use of synthetic dyes is indispensable as such dyes are cheap, stable, and are readily available in large quantities. Moreover, synthetic dyes provide a wide range of vibrant colors and shades, surpassing those of natural dyes. Industries that are responsible for dye contaminated wastewater include textile, paper and pulp, tannery and paint, dye manufacturer, dyeing industries, and many others. Of these, the textile industry is the main contributor to more than 50% of the current dye effluents present in wastewater today [1]. Not only are dye contaminated water an eye-sore due to strong colors, they also produce an unpleasant odor, and deter sunlight penetration which in turn disrupt photosynthesis of aquatic plants. Being stable with complex structures, these dyes are not easily degradable and are able to withstand various conditions, such as heat, light, and oxidizing agents. Hence, once the water bodies are being contaminated with persistent dyes, the whole ecosystem will be very much affected. The contaminated dye wastewater spreads along the food chain and being toxic and carcinogenic, humans are at risk of being

* Corresponding author.

affected by these harmful dyes [2]. Methyl violet 2B (MV) dye, an organic compound of intense color belonging to the triphenylmethane dyes, as shown in Fig. 1, is one example of such harmful dyes being used in print inks and paints. MV is also used in textiles in the dyeing of silk, cotton, and leather. Apart from that, MV is used as classification of bacteria as it has the ability to stain Grams bacteria. Despite many uses, MV has been found to cause irritation when ingested or inhaled.

Over the years, a number of methods have been used to treat wastewater [1]. Of these, one of the simplest and direct methods is via adsorption. Not only does it not require high skills and complicated operation, adsorption is also superior in terms of its simplicity in design, economy, efficiency, and flexibility. Many different types of adsorbents have been successfully utilized to adsorb dyes and these include minerals [3,4], industrial wastes [5–7], aquatic plants [8], agricultural wastes [9–11], fruit wastes [12–17], and many others [18–22]. Not all adsorbents are able to remove dyes efficiently. Adsorption characteristics of an adsorbent depends on various factors such as its surface area, porosity, as well as its ability to retain its adsorption capacity when there are changes in the environment, for example, under varying conditions of pH and ionic strength, etc. Hence, there is a need to discover and develop better and more effective adsorbents. As such, the emergence of adsorbents including modified adsorbents [23–27] and synthetic materials [28,29] to cater for these needs has been observed in the recent past. Surface modification by chemical means using acids, bases, surfactants, etc., has gain popularity owing to its simplicity which usually involves single-step process and does not require high temperature. Chemical modification offers a wide range of advantages such as the enhancement of porosity of the adsorbent's surface together with increased active binding sites, possibility of introducing more functional groups, and altering the surface charge, all of which would improve the extent of adsorption of the adsorbent [30].

Leaf-based adsorbents have gained popularity in recent years due to being easily available and abundant throughout the year. The presence of a variety of compounds, such as cellulose, lignin, and pectin, can also aid in the adsorption process [19]. To date, the use of pomelo as an adsorbent is largely from utilizing the skin [31–33], whilst limited reports were based on its leaves to remove adsorbates [34,35]. This work aims to prepare NaOH modified pomelo leaves (NaOH-PL) as the adsorbent in order to evaluate if simple chemical modification could enhance its adsorption toward MV dye (Fig. 1). Investigation into the adsorption characteristics of NaOH-PL will be presented, which include isotherm and kinetics of the adsorption process. The influence of pH and salt concentration on the adsorption of MV by NaOH-PL as well as the ability to regenerate and reuse the spent adsorbent will also be studied.

2. Methods and materials

2.1. Preparation of modified adsorbent and chemical reagents

Dried pomelo leaves (PL) collected from the ground of backyard home garden were washed with distilled water several times, allowed to air-dry under sunlight, and placed in an oven at 65°C until a constant mass was obtained. Dried PL samples were blended using a household blender and sieved using a stainless steel sieves apparatus in order to acquire particles of diameter <355 μm. For chemical modification, PL powder (50.0 g) was soaked in 1.0 M NaOH (1,000 mL) solution for 2.0 h with constant stirring to mix well. After stirring, base-modified adsorbents (NaOH-PL) were washed with distilled water until neutral pH was obtained, and dried in an oven at 65°C to a constant mass. NaOH-PL powder was then stored in an airtight plastic bag until ready to be used. Methyl violet 2B (MV) dye was selected as an adsorbate to be removed by NaOH-PL adsorbent in adsorption studies. MV 2B dye (purity 80%) with the molecular weight of 393.96 g mol^{-1} and molecular formula of $C_{23}H_{26}N_3Cl$ was purchased from Sigma-Aldrich Corporation, (Germany).

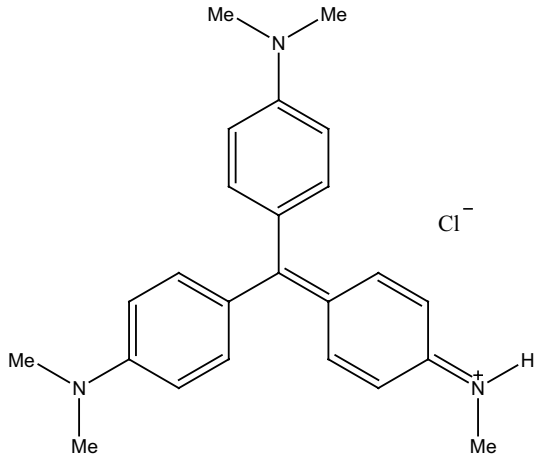

Fig. 1. Chemical structure of methyl violet 2B dye.

2.2. Adsorption experiment methods

In this research, the extent of removal of MV dye via NaOH-PL was determined by investigating the effects of contact time [0–150 min; at every 30 min interval], medium pH [2–12], ionic strength [0–1 M NaCl] as well as batch adsorption isotherm [0–1,000 mg L^{-1}] following the methods reported by Lim et al. [36]. Adsorption kinetics experiments using 100 mg L^{-1} dye were carried out at 1 min interval for the first 10 min; thereafter at 3 min intervals up to 30 min followed by 10 min intervals up to 60 min, and finally at 30 min intervals from 60 to 150 min. In addition, regeneration study for NaOH-PL was carried out for five consecutive cycles, using 0.1 M HCl, 0.1 M NaOH, and distilled water treatment for the desorption of MV dye, and also a control experiment for comparison, following the procedure as described by Lim et al. [37]. Briefly, dried NaOH-PL loaded with MV dye (spent adsorbent) was divided into four portions, to be treated with acid, base, and distilled water with the last portion as the control. After treatment, the samples were filtered and dried overnight in an oven at 65°C and then shaken with MV dye for the desired contact time. This is considered as one cycle and the process was repeated for five consecutive cycles.

2.3. Instrumentation

The adsorbate-MV mixtures were agitated using the Stuart SSL1 orbital shaker, UK, set to 250 rpm. The Thermo Scientific Genesys 20 UV-Visible spectrophotometer, USA, was used to measure the absorbance of MV dye at the wavelength of 584 nm. Infrared spectra of NaOH-PL, before and after adsorption of MV dye, were recorded using Fourier transform infrared spectroscopy (FTIR, Model: Agilent Cary 630 FTIR spectrometer, USA). Surface morphology images were taken using the Quanta 400, FEI, scanning electron microscopy (SEM, Czech Republic). Solution pH was measured using the EDT instruments GP353 ATC pH meter, UK.

3. Results and discussion

3.1. Surface characterization using scanning electron microscopy

Scanning electron microscopic (SEM) imaging of untreated PL, shown in Fig. 2a, appears relatively flat, without many pores on the surface. However, the SEM image after base treatment of PL, illustrated in Fig. 2b, shows a very distinct change to the surface morphology. The stomata on the surface are clearly visible, shown by the red circles in Fig. 2b, and the surface is more undulating with more folds. This is probably due to NaOH having the ability to strip off the surface fats and waxes, thereby exposing functional groups such as hydroxyl and amino groups in the underlying surface of PL where mesophyll cells containing chloroplasts are present. Upon adsorption of MV dye, Fig. 2c shows that these stomata are no longer visible and the surface of MV loaded NaOH-PL is altered, showing a much rougher and more irregular surface.

3.2. Functional group characterization

Chemical modification of PL with NaOH showed distinct shifts in some of the peaks, as shown in Fig. 3a. Prior to base treatment, C–H stretching present in aromatic methoxy group and the methyl and methylene groups of side chains appeared at 2,918 and 2,850 cm^{-1} [38]. Upon treatment of PL with NaOH, major changes were observed for peaks in the region of 2,500 to 3,600 cm^{-1} with a prominent broad O–H peak at 3,346 cm^{-1}. Similarly, the C=O and C=C peaks of PL at 1,781 and 1,619 cm^{-1} were shifted to 1,800 and 1,631 cm^{-1}, respectively. Such observation is in line with the fact that base modification can remove some of the surface waxes and fats, and at the same time, deprotonate some functional groups on the surface of the adsorbent. Adsorption of MV dye on NaOH-PL also caused the relevant functional groups involved to be shifted, as shown in Fig. 3b, especially within the region of 3,000–3,600 cm^{-1} indicating the involvement of O–H and N–H in the adsorption process. Also involved was the C=O functional group which upon adsorption of MV was shifted to 1,787 cm^{-1}.

3.3. Effect of contact time on MV adsorption

One important parameter in adsorption studies is the time required for the adsorbent-adsorbate system to reach equilibrium. With this information, it enables proper planning and design of the adsorption system. Investigation of the contact time, shown in Fig. 4, shows that the uptake of MV dye by NaOH-PL was fast, reaching >80% within the first 30 min. Thereafter, the percentage removal of dye did not show a large variation over the 4-h period of contact time studied. The data observed can be explained by the initial availability of vacant sites on the adsorbent's surface which allows fast adsorption of MV dye molecules to take place. As more of these sites are being filled, less dye molecules are able to get adsorbed, and hence, the observed levelling to a plateau. A fast contact time for the adsorbent-adsorbate system to reach equilibrium is a desirable factor in an adsorption process. Not only does it indicate the trait of a potentially good adsorbent, the short time period of adsorption will also be more cost effective in terms of design and application of wastewater treatment.

3.4. Kinetics of adsorption of MV on NaOH-PL

Kinetics study was carried out to help provide information and more clearly understand from the adsorption mechanistic point of view. The experimental data were therefore fitted using two models, namely the Lagergren pseudo-first-order [39] and the pseudo-second-order [40] models, whose nonlinear and linearized equations are shown in Table 1. Both these models have been widely used in adsorption kinetics studies [41]. Error analyses were also carried out using four error functions, shown in Eqs. (1)–(4).

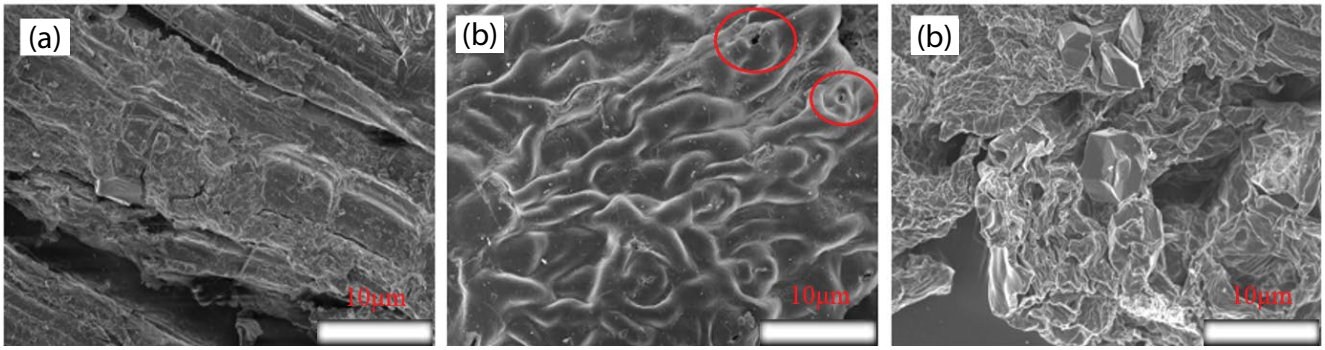

Fig. 2. SEM images of (a) untreated PL, (b) NaOH-PL, and (c) NaOH-PL after adsorption of MV dye (×850 magnifications).

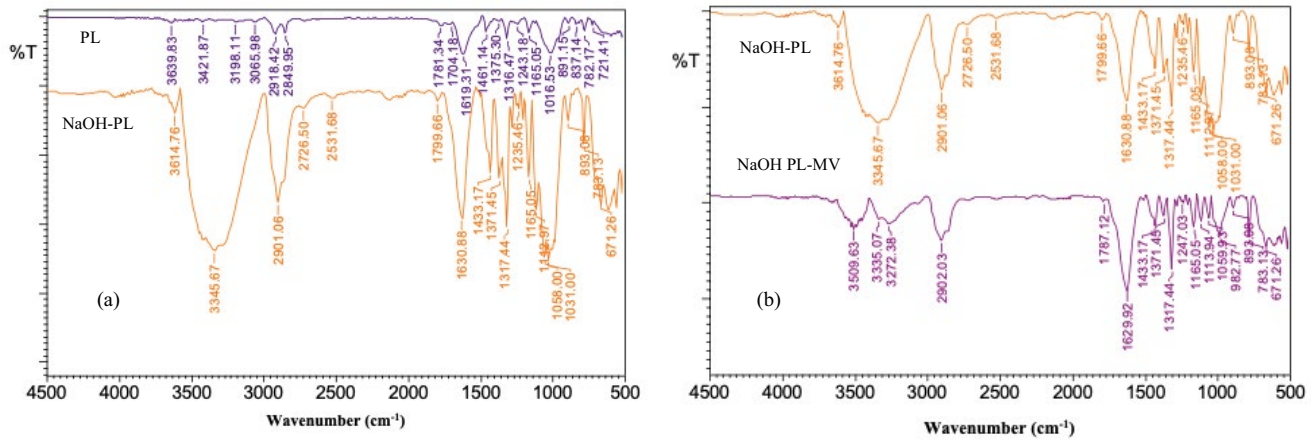

Fig. 3. Infrared spectra of (a) PL (Blue) and NaOH PL (Orange) and (b) NaOH PL (Orange) and NaOH PLMV (Purple).

Table 1
Comparison of nonlinear and linear analyses of the Lagergren pseudo-first-order and pseudo-second-order kinetic models and their error values

Kinetics model	Nonlinear	Linear
Pseudo-first-order	$q_t = q_e\left(1-e^{-k_1 t}\right)$	$\log\left(q_e - q_t\right) = \log\left(q_e\right) - \frac{k_1}{2.303}t$
q_{calc} (mmol g^{-1})	0.099	0.032
k_1 (min^{-1})	0.410	0.023
R^2	0.9540	0.7881
ARE	6.980	87.091
SSE	0.001	0.132
EABS	0.120	1.689
χ^2	0.012	1.463
Pseudo-second-order	$q_t = \frac{q^2 e^{k_2 t}}{1+\left(k_2 q_t t\right)}$	$\frac{t}{q_t} = \frac{1}{k_2 q_e^2} + \frac{1}{q_e}t$
q_{calc} (mmol g^{-1})	0.106	0.111
k_2 (g mmol^{-1} min^{-1})	5.679	2.844
R^2	0.9995	0.9967
ARE	2.816	12.020
SSE	0.0002	0.003
EABS	0.051	0.235
χ^2	0.002	0.037
q_{expt} (mmol g^{-1})	0.103	

k_1 and k_2 are the rate constants of the pseudo-first-order and pseudo-second-order kinetics, respectively; t is reaction time; q_e and q_t represent the adsorption capacity at equilibrium and at time t, respectively.

Average relative error (ARE):

$$\frac{100}{n}\sum_{i=1}^{n}\left|\frac{q_{e,\text{meas}} - q_{e,\text{calc}}}{q_{e,\text{meas}}}\right|_i \quad (1)$$

Sum square error (SSE):

$$\sum_{i=1}^{n}\left(q_{e,\text{calc}} - q_{e,\text{meas}}\right)_i^2 \quad (2)$$

Sum of absolute error (EABS):

$$\sum_{i=1}^{n}\left|q_{e,\text{meas}} - q_{e,\text{calc}}\right| \quad (3)$$

Non-linear chi-square test (χ^2):

$$\sum_{i=1}^{n}\frac{\left(q_{e,\text{meas}} - q_{e,\text{calc}}\right)^2}{q_{e,\text{meas}}} \quad (4)$$

Linear plots of the Lagergren pseudo-first-order and the pseudo-second-order, as shown by Figs. 5a and b, respectively indicated that the former model gave much lower R^2 whilst the R^2 of the pseudo-second-order is higher and very close to unity, as seen from Table 1. Further, the Lagergren pseudo-first-order has much higher overall error values. This can be further confirmed by the plots in Fig. 5c in which the pseudo-first-order deviated from the experiment data obtained, while the pseudo-second-order kinetics, on the other hand, shows a much better fit and its q_{expt} was also very close to the q_{calc} value.

In this study, the nonlinear regression of the kinetics models was also analyzed using the Microsoft Excel with solver add-in, whilst minimizing error function. Although from Fig. 5d, both kinetics models were close to the experimental data, the pseudo-second-order appeared closer to the experimental data. The error values also indicated that the Lagergren pseudo-first-model has much higher overall errors. The q_{calc} and q_{expt} values of pseudo-second-order, as shown in Table 1, matched very well but this is not the case for Lagergren pseudo-first-order kinetics. The lower R^2 obtained from nonlinear regression fitting further confirms that the Lagergren pseudo-first-order is not the correct model to describe the adsorption kinetics of this system.

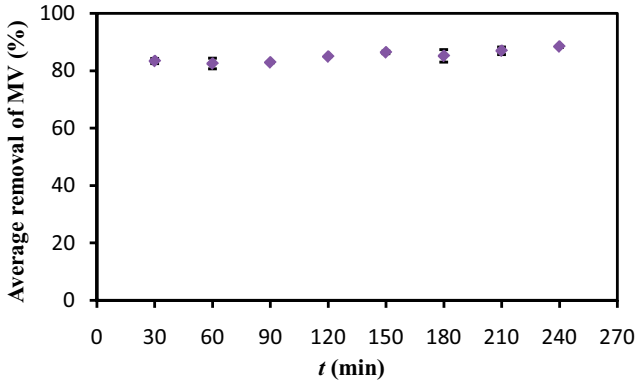

Fig. 4. Effect of shaking time for the removal of MV by NaOH-modified PL (mass of adsorbent = 0.020 g; volume of MV solution = 10.0 mL; concentration of MV = 100 mg L^{-1}).

Validity of pseudo-second-order kinetics for adsorption of MV on NaOH-PL suggests that the adsorption process would involve electrostatic forces between dye molecules and adsorbent's functional groups, and that the adsorption could be chemisorption. It is interesting to note that overall, the nonlinear regression is better than the linear analyses for adsorption kinetics since the former gave significantly lower error values. The rate constant k_2 for NaOH-PL, based on non-linear regression fitting, was found to be 5.679 g $mmol^{-1}$ min^{-1}, which is faster than that was reported for the unmodified PL where k_2 was 4.258 g $mmol^{-1}$ min^{-1} [34], showing NaOH-PL to be more efficient in the removal of MV dye.

Adsorption of adsorbate on surface-active sites of an adsorbent is usually a complex process where more than one mechanism may be involved. First, the adsorbate molecules have to overcome the boundary layer effect, followed by diffusion from the boundary layer film on the active sites on the surface of the adsorbent. Thereafter, diffusion into the pores of the adsorbent can occur, and eventually final equilibrium is reached. Since both the Lagergren pseudo-first-order and the pseudo-second-order kinetics models do not give insight into diffusion, kinetics data obtained were

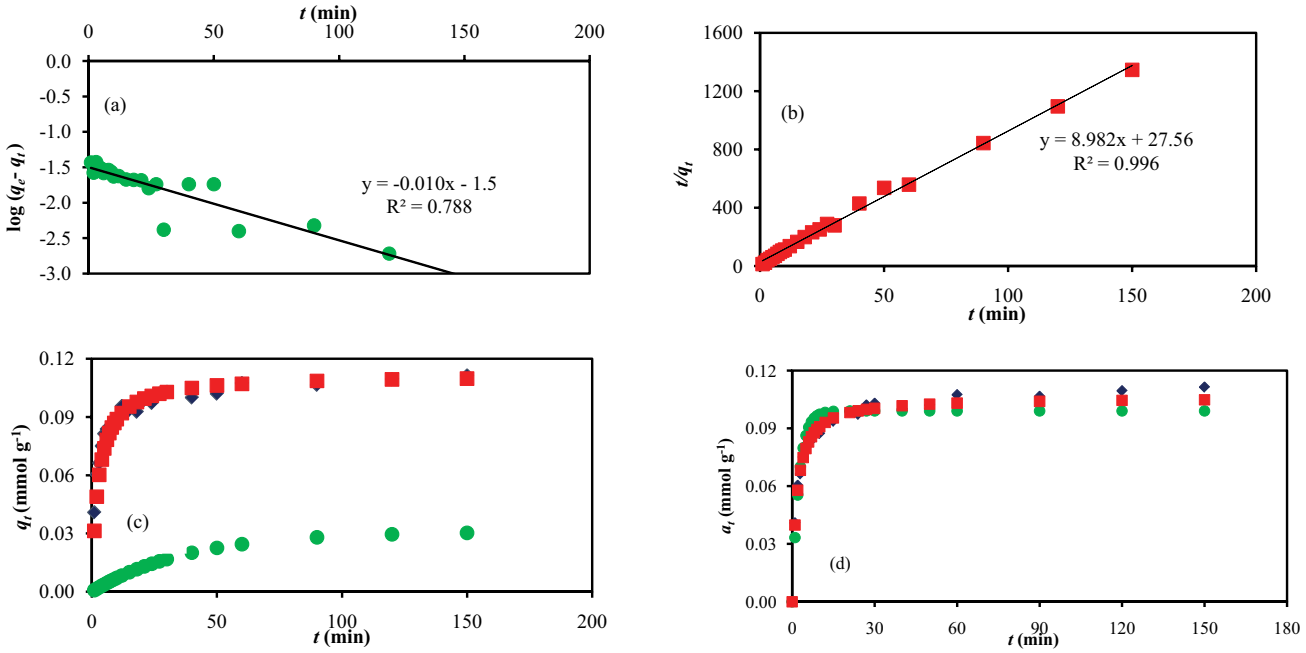

Fig. 5. Adsorption kinetics of NaOH-PL for MV removal (a) linear plot of pseudo-first-order, (b) linear plot of pseudo-second-order, (c) comparison of simulation plots based on linear, and (d) non-linear regression of pseudo-first-order (●) pseudo-second-order (■) and experiment data (◆) (mass of adsorbent = 0.020 g, volume of MV solution = 10.0 mL, and concentration of MV = 100 mg L^{-1}).

fitted to the Weber–Morris intraparticle diffusion model [42], represented in Eq. (5). It is assumed in this model that if the plot passes through the origin, intraparticle diffusion is the only rate-controlling step; otherwise there will be some degree of contribution from the boundary layer diffusion.

$$q_t = k_i t^{\frac{1}{2}} + C \quad (5)$$

where k_i is the intraparticle diffusion constant (mg g^{-1} min^{-1}) and C depicts the boundary layer effect (mg g^{-1}).

As observed from Fig. 6a, the adsorption takes place in different stages, suggesting that different mechanisms be involved and that intraparticle diffusion may not be the only rate controlling step. At the onset of the adsorption, the boundary layer diffusion of adsorbates onto active sites on the surface of the adsorbent was fast, as shown by the steepest slope. Thereafter, intraparticle diffusion into the mesopores of the adsorbent takes place and finally into the micropores until equilibrium is reached [43]. The non-linear regression fitting, as shown in Fig. 6b, does not show a very good fit of this model.

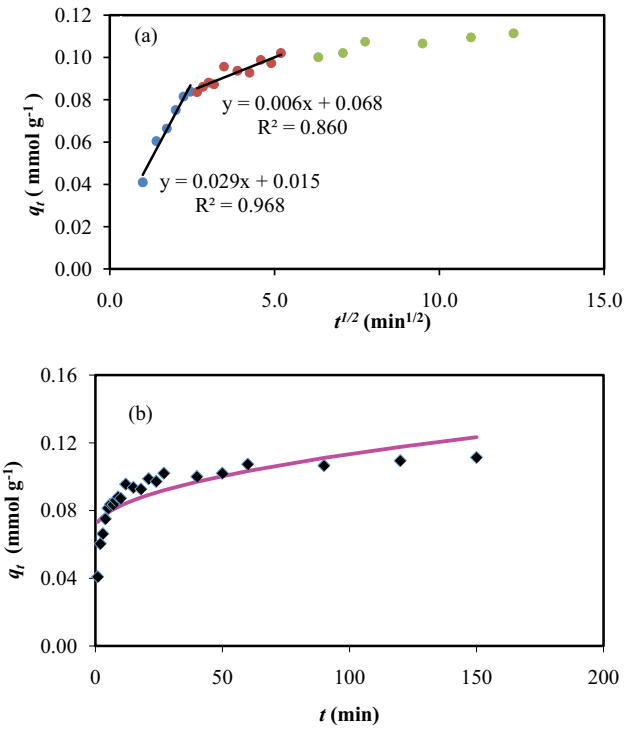

Fig. 6. (a) The Webber–Morris intraparticle diffusion model plot (mass of adsorbent = 0.020 g; volume of MV solution = 10.0 mL) and (b) comparison of the experiment data (◆) and non-linear regression fitting of the Webber–Morris intraparticle diffusion (▬).

3.5. Adsorption isotherms

An important study in any adsorption process involves the investigation of adsorption isotherms by fitting experimental data to different models which will help to provide understanding into the surface properties of the adsorbent and its relation to the adsorbate. The maximum adsorption capacity (q_{max}) obtained through such models would help shed light on the performance of the adsorbent being investigated, that is, its applicability in real wastewater treatment. In this study, five adsorption isotherm models were employed, namely Langmuir [44], Freundlich [45], Temkin [46], Redlich–Peterson (R–P) [47], and Sips [48] models (Table 2).

In order to select which of these five isotherm models best fit the adsorption of MV onto NaOH-PL, both linear and nonlinear regression fittings of the models were employed and the results were compared. To date, many adsorption studies have widely utilized the linear regression analysis since this method is relatively simple and straight forward when compared to the nonlinear regression analysis [16,26]. However, in an attempt to narrow the experimental and predicted data and owing to its better fit, the use of nonlinear regression analysis is becoming increasingly popular [49]. In this study, selections of the best isotherm model were based on three selection criteria: highest R^2 value, lowest error values using four different error functions, and comparison of experiment data with simulation plots of the five isotherm models.

3.5.1. Linear regression analyses of isotherm models

Despite its reasonable R^2 value, the Temkin model has the highest overall error values and Fig. 7a also indicated that this model far deviated from the experiment data. Hence, the Temkin model was ruled out. Although the error values of the Langmuir and Redlich–Peterson models were reasonable, they have the lowest $R^2 < 0.66$ (Table 3). Hence, both models are not the best fit models to describe the adsorption process.

Both the Freundlich and Sips models have high $R^2 > 0.977$. The Freundlich model is indicative of a multilayer adsorption on heterogeneous surface of the adsorbent. The value n in the Freundlich model is the adsorption constant that could provide information on the strength of adsorption. The adsorption process is considered unfavourable if $1/n > 1$, favourable when $0 < 1/n < 1$ and irreversible if $1/n$ is zero. In this study, the value of $1/n$ is 0.82, indicating a favourable adsorption process. Between the Freundlich and Sips models, the latter has lower overall error values. In fact, the Sips model is sometimes known as the Langmuir–Freundlich model, showing characteristics of the Freundlich at low adsorbate concentration. Comparison of these two models with the experiment data, as shown in Fig. 7a, also indicates that the Sips model is more suitable.

3.5.2. Nonlinear regression analyses of isotherm models

As with the nonlinear regression, the Temkin model can be ruled out based on its lowest R^2, highest error values (Table 3), and further, Fig. 7b clearly shows that this model deviated from the experiment isotherm data. Unlike the linearized isotherm results where the Sips was the best model, the nonlinear regression analysis showed that even though the Sips has good R^2 close to unity, its overall error values, presented in Table 3, were the second highest after

Table 2
Nonlinear and linearized equations of the five adsorption isotherm models used in this study

Non-Linearized Equation	Linearized equation	Plot
Langmuir		
$q_e = \frac{Q_m K_L C_e}{1 + K_L C_e}$	$\frac{C_e}{q_e} = \frac{1}{K_L q_{\max}} + \frac{C_e}{q_{\max}}$	$\frac{C_e}{q_e}$ vs. C_e
C_e and q_e are the concentration and adsorption capacity at equilibrium, respectively; K_L is the Langmuir constant and $q_{\max}$ is the maximum adsorption capacity		
Freundlich		
$q_e = K_F C_e^{\frac{1}{n}}$	$\log q_e = \frac{1}{n}\log C_e + \log K_F$	$\log q_e$ vs. $\log C_e$
K_F is the Freundlich constant indicative of adsorption capacity; n is related to the adsorption intensity		
Temkin		
$q_e = \frac{RT \ln\left(K_T C_e\right)}{b_T}$	$q_e = \left(\frac{RT}{b_T}\right)\ln K_T + \left(\frac{RT}{b_T}\right)\ln C_e$	q_e vs. $\ln C_e$
K_T is the Temkin constant; b_T is related to the heat of adsorption; R is the gas constant while T is the absolute temperature at 298 K		
Redlich–Peterson		
$q_e = \frac{K_R C_e}{1 + \alpha_R C_e^n}$	$\ln\left(\frac{K_R C_e}{q_e} - 1\right) = n \ln C_e + \ln a_R$	$\ln\left(\frac{K_R C_e}{q_e} - 1\right)$ vs. $\ln C_e$
K_R and a_R are the R–P constants and n is the empirical parameter related to the adsorption intensity		
Sips		
$q_e = \frac{q_m K_s C_e^{\frac{1}{n}}}{1 + K_s C_e^{\frac{1}{n}}}$	$\ln\left(\frac{q_e}{q_{\max} - q_e}\right) = \frac{1}{n}\ln C_e + \ln K_s$	$\ln\left(\frac{q_e}{q_{\max} - q_e}\right)$ vs. $\ln C_e$
K_S is the Sips constant; n is the Sips exponent		

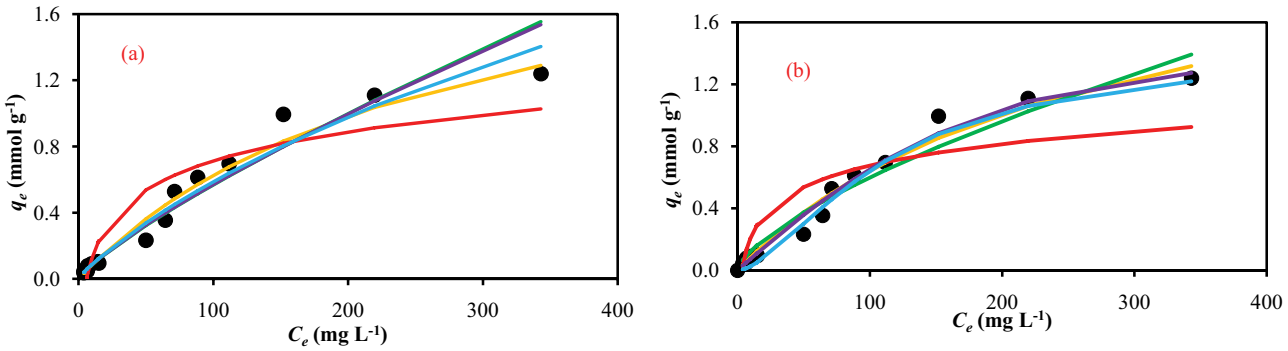

Fig. 7. (a) Linear and (b) nonlinear regression plots of different adsorption isotherm models compared with the experiment data obtained (experiment (•), Langmuir (), Freundlich (), Temkin (), R–P (), and Sips () (mass of adsorbent = 0.020 g; volume of MV solution = 10.0 mL; concentration of MV = 0–1,000 mg L^{-1}).

the Temkin model. Of the three models left, the Freundlich isotherm has the lowest R^2 and overall higher error values. This is further confirmed from Fig. 7b, where deviation from the experiment data can be seen. Between the Langmuir and Redlich–Peterson models, the latter is the best owing to its slightly higher R^2 and lower error values.

The Redlich–Peterson model, like the Sips model, is a three-parameter isotherm model having features of both the Langmuir and Freundlich isotherms. At high adsorbate concentrations, the Redlich–Peterson reduces to the Freundlich, whilst at low adsorbate concentrations it will tend toward the Langmuir isotherm. This model is versatile in that it can be applied to both homogeneous and heterogeneous adsorbents.

However, it must be highlighted that unlike the kinetics where there was a clear cut that the nonlinear regression

Table 3
Comparison of linear and nonlinear adsorption parameters and error values of the five isotherm models used

Isotherm model and parameters	Nonlinear	Linear
Langmuir		
q_{max} (mmol g^{-1})	2.312	2.290
K_L (L mmol^{-1})	0.004	0.004
R^2	0.9617	0.6559
ARE	17.01	17.67
SSE	0.06	0.07
EABS	0.68	0.72
χ^2	0.17	0.16
Freundlich		
K_F (mmol g^{-1} (L mmol^{-1})$^{1/n}$)	0.026	0.013
n	1.461	1.224
R^2	0.8983	0.9774
ARE	30.96	17.01
SSE	0.12	0.17
EABS	1.08	1.04
χ^2	0.31	0.22
Temkin		
K_T (L mmol^{-1})	0.288	0.165
b_T (kJ mol^{-1})	12.31	9.734
R^2	0.7709	0.8587
ARE	71.67	96.12
SSE	0.48	0.37
EABS	2.18	2.07
χ^2	1.85	2.27
Redlich–Peterson		
K_R (L g^{-1})	0.008	0.040
α	1.549	0.225
a_R (L mmol^{-1})	0.0001	2.137
R^2	0.9760	0.6851
ARE	15.90	17.12
SSE	0.04	0.16
EABS	0.56	1.02
χ^2	0.14	0.21
Sips		
q_{max} (mmol g^{-1})	1.412	5.000
K_S (L mmol^{-1})	0.0005	0.002
n	0.611	1.144
R^2	0.9986	0.9773
ARE	35.59	16.89
SSE	0.05	0.10
EABS	0.72	0.90
χ^2	0.30	0.17

method gave lower overall errors compared to the linearized models, this is not so for all the isotherm models. For example, ARE and χ^2 for the Sips model showed smaller errors for linearized analyses. Further, its simulation plot, as shown in Fig. 7b, also indicated its closeness to the actual experiment isotherm data. Therefore, it could still be a valid model.

Maximum adsorption capacity (q_{max}) of NaOH-PL, according to the linear regression, based on the Sips model is 1.970 × 10^3 mg g^{-1} (5.00 mmol g^{-1}), while the monolayer adsorption based on the Langmuir model in the nonlinear regression analysis has a value of 2.312 mmol g^{-1} (910.8 mg g^{-1}) (Table 3). The untreated PL was reported to have q_{max} of 248.2 mg g^{-1} [34]. Thus, base modification of PL was able to successfully enhance its adsorption capacity significantly. This is most likely due to base being able to expose functional groups for better adsorption with the dye molecules. Deprotonation of functional groups by base treatment forming negatively charged surface moieties would result in stronger electrostatic attractions toward cationic MV dye making another contribution to enhanced absorption characteristics.

Various adsorbents have emerged in recent years, including natural, modified and synthesized adsorbents, in the hope to enhance and improve the performance of the adsorbents [50–52]. However, not all adsorbents, be it synthesized or modified, showed good adsorption capacity. For example, palm kernel, almond shell, and mangrove leaf upon modification showed <30% improvement in its adsorption capacity (Table 4). When compared to many synthesized and modified adsorbents, NaOH-PL is much superior as an adsorbent toward MV dye.

3.6. Point of zero charge of NaOH-PL and the effect of pH on adsorption of MV

Knowledge on the point of zero charge (pH_{Pzc}) of an adsorbent can provide useful information and help predict how the adsorbent behaves when placed in solutions of different pH. The pH of a solution usually has a significant influence on the adsorption process since pH can alter the chemical characteristics of both the adsorbent and adsorbate. The pH_{Pzc} denotes the pH at which the surface of an adsorbent has zero charge. Below this pH, protonation of the functional groups on the surface of the adsorbent can occur, resulting in the overall surface to be predominantly positively charged. When pH > pH_{Pzc}, the surface would be expected to be predominantly negatively charged as a result of deprotonation of these functional groups. The pH_{Pzc} of NaOH-PL was determined from the plot of DpH vs. initial pH, as shown in Fig. 8a. Compared to PL, whose pH_{Pzc} was reported to be at pH 5.02 [34], base modification has increased the pH_{Pzc} of NaOH-PL to pH 7.18, and therefore become more basic. Similar shifts were also reported for the NaOH modified Cassava peel (pH_{pzc} 7.02) [74] and *Artocarpus odoratissimus* leaves (pH_{pzc} 7.9) [75].

Maximum adsorption of MV was observed at pH 12, as shown in Fig. 8b, attributing to the predominantly negative charged surface being attracted to the cationic MV dye molecules. Under strong acid medium at pH 2 where high concentration of H_3O^+ ions are in competition with cationic MV dyes for active sites, adsorption was drastically reduced by approximately 55%. Further, protonation of surface functional groups at pH < pH_{Pzc} will cause repulsion with the cationic MV dye. When pH > pH_{Pzc}, negatively charged

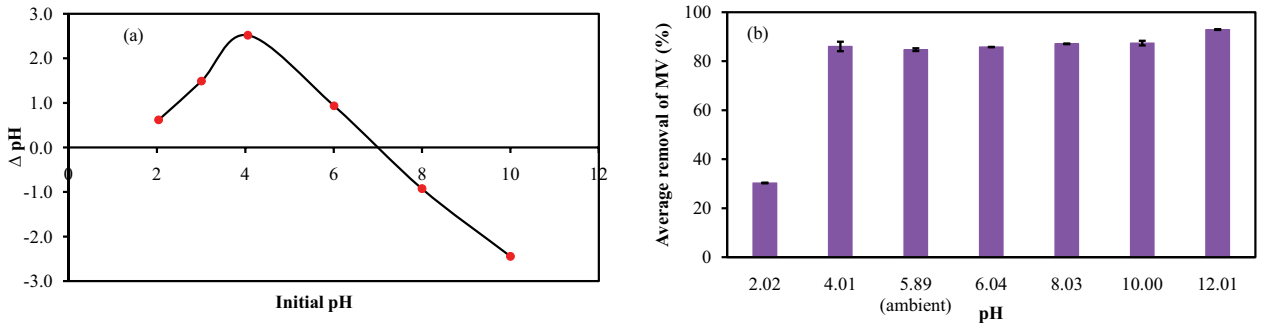

Fig. 8. (a) Determination of pH_{Pzc} of NaOH-PL and (b) effect of medium pH on adsorption of MV onto NaOH-PL (mass of adsorbent = 0.020 g, volume of MV solution = 10.0 mL, and concentration of MV = 100 mg L^{-1}).

Table 4
List of selected adsorbents (natural, modified, or synthesized) and their q_{max} values

Adsorbent	q_{max} (mg g^{-1})	Reference
NaOH modified Pomelo leaf	910.8	This study
Pomelo leaf	248.2	[34]
Pomelo skin	468.3	[31]
Palm kernel activated carbon	83.9	[53]
Modified palm kernel	107.3	[53]
Almond shell	29.4	[54]
Magnetite impregnated almond shell	33.0	[54]
Sapindus mukorossi (reetha) pericarp	30.6	[55]
Mangrove leaf	78.0	[56]
Chemically modified mangrove leaf	98.5	[56]
Uncalcined Cu/Al layered double hydroxide	361.0	[57]
Halloysite-magnetite-based composite (HNT–Fe_3O_4)	20.0	[58]
Artocarpus odoratissimus leaves	139.7	[59]
NaOH modified *Artocarpus odoratissimus* leaves	1,004.3	[59]
C. camphora leaves powder	104.2	[60]
NaOH modified *C. camphora* leaves powder	206.6	[61]
Activated Phragmites karka	371.6	[62]
Granulated mesoporous carbon	202.8	[63]
Hyperbranched polyglycerol poly(acrylic acid) hydrogel	394.1	[64]
Lemna minor (Duckweed)	419.8	[65]
Acid modified *Saccharum bengalense*	7.3	[66]
Egg shell microparticles	83.1	[67]
Egg shell nanoparticles	123.5	[67]
Unmodified cellulose	43.7	[68]
Modified cellulose	106.4	[68]
Artocarpus odoratissimus stem axis	263.7	[69]
Cucumis melo var cantalupensis (rock melon) skin	224.6	[70]
NaOH modified rock melon skin	669.7	[70]
Modified nano-graphite/Fe_3O_4 composites	144.7	[71]
Synthesized carbon nanospheres	395.0	[72]
Poly-melamine-formaldehyde	113.9	[73]

adsorbent surface would favor adsorption of the cationic MV dye. Apart from pH 2, all other medium pH values do not seem to have much adverse effects on the adsorbent toward its removal of MV. NaOH-PL is therefore relatively unaffected by changes in pH, apart from pH 2 which is a strong acidic medium which would not be used in practical situations. Since the removal of MV is good and comparable even under untreated (ambient) pH, no adjustment

of pH was deemed necessary and all experiments in this study were thus carried out under ambient pH.

3.7. Ionic strength effect on the adsorption of MV by NaOH-PL

A good adsorbent should be able to maintain its adsorption ability and withstand changes in the environment conditions. One such condition is when the adsorbent is present in solutions of different ionic concentrations (strengths). This is because dye effluents usually contain salts which may influence the adsorption process. For example, the metal ions present may compete with cationic dye molecules for active sites. Further, NaCl is one of the salts often used in dyeing process. Being economical and readily available, NaCl is often added to promote fixation and affinity of dyestuff onto the fibre. Hence in this study, NaCl was chosen as the selected salt to investigate ionic strength effect. NaOH-PL was investigated for its adsorption ability when placed in various concentrations of NaCl ranging from 0 to 1 mol dm^{-3}. Although there was an observed decrease trend in the removal of MV (Fig. 9), NaOH-PL was still able to remove approximately 70% MV in the presence of 1.0 M NaCl, indicating that NaOH-PL is relatively unaffected by ionic strength.

3.8. Regeneration of NaOH-PL

For an adsorbent to be considered applicable in wastewater treatment, one important criterion that should be met is its ability to be regenerated and reused. Otherwise, inefficiency of the adsorbent will result in higher operation cost since the spent adsorbent has to be discarded each time after being used. Reusability of NaOH-PL that has been used for adsorption of MV dye, that is, spent NaOH-PL was tested in this research with three treatment methods (0.1 M HCl, 0.1 M NaOH, and distilled water) together with a control. The spent NaOH-PL analysed for its adsorption of MV over five consecutive cycles showed very promising results, as presented in Fig. 10. NaOH-PL demonstrated its ability to be reused and regenerated, while maintaining excellent adsorption even at the fifth cycle, with the order of base > acid > control > water. The control experiment showed that the spent NaOH-PL could still adsorb approximately 70% MV at the fifth cycle, whilst base and acid treatment maintained adsorption of 85% and 87%, respectively. Daneshvar et al. [76] tested out 17 different eluents in cationic dye desorption and of these, HCl gave the highest desorption efficiency. They attributed this to an increase in electrostatic repulsion between positively charged active sites on the adsorbent's surface and cationic dye molecules, as well as the possible increase of adsorbed cationic dyes being replaced by H^+ ions. On the other hand, washing with base has the ability to remove surface waxes and fats thereby unveiling functional groups for better adsorption [77]. The ability for NaOH-PL to be regenerated and reused, with or without treatment methods, is favourable in terms of wastewater treatment application. Many spent adsorbents have been reported to show drastic decrease in their adsorption capacity when no treatment methods were applied [78,79].

4. Conclusion

Pomelo leaves, a natural adsorbent which is readily available in large quantity throughout the year, have been successfully modified with NaOH. Through this simple one-step modification process, which required no heating, the adsorption capacity of the modified adsorbent was greatly enhanced by approximately eight times. When compared to many reported adsorbents, including those modified or synthesized adsorbents requiring complicated processes, NaOH-PL illustrated much superior adsorption ability toward MV dye. Another attractive feature of it being a potential adsorbent in wastewater treatment is its ability to regenerate and reuse, whilst maintaining high adsorption of >85% even after five consecutive cycles under both acid and base treatment. The spent NaOH-PL could also be reused after the fifth cycle without any treatment, giving approximately 70% dye removal, indicating it is technically feasible and economical in practical applications. NaOH-PL's ability to withstand various environment conditions such as pH and ionic strength while maintaining good adsorption capacity further supports its application as a promising low-cost adsorbent in wastewater treatment. Fast adsorption time is another desirable feature since if applied to wastewater treatment, this will minimize cost with maximum

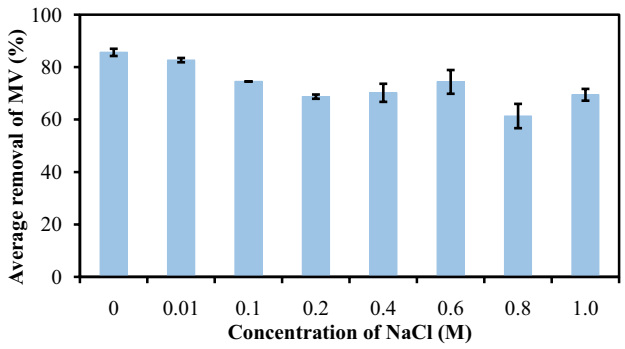

Fig. 9. Effect of NaCl concentration for the removal of MV by NaOH PL (mass of adsorbent = 0.020 g, volume of MV solution = 10.0 mL, and concentration of MV = 100 mg L^{-1}).

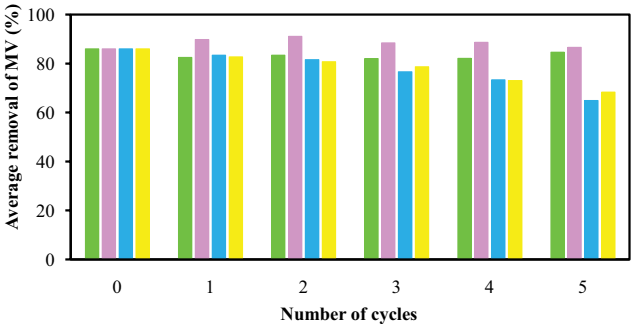

Fig. 10. Regeneration of spent NaOH PL for the removal of MV throughout five consecutive cycles using acid (■), base (■), water (■), and control (■) (mass of adsorbent = 0.020 g; concentration of MV = 100 mg L^{-1}).

profitability and output. Undoubtedly, the above findings support NaOH-PL as a promising adsorbent in terms of wastewater treatment and commercial application.

Acknowledgments

The authors would like to thank the Government of Brunei Darussalam and the Universiti Brunei Darussalam (UBD) for their continuous support. We sincerely thank the Physical and Geological Sciences Program at UBD for the use of SEM.

References

[1] V. Katheresan, J. Kansedo, S.Y. Lau, Efficiency of various recent wastewater dye removal methods: a review, J. Environ. Chem. Eng., 6 (2018) 4676–4697.
[2] A. Tkaczyk, K. Mitrowska, A. Posyniak, Synthetic organic dyes as contaminants of the aquatic environment and their implications for ecosystems: a review, Sci. Total Environ., 717 (2020) 137222.
[3] H. Aghdasinia, H.R. Asiabi, Adsorption of a cationic dye (methylene blue) by Iranian natural clays from aqueous solutions: equilibrium, kinetic and thermodynamic study, Environ. Earth Sci., 77 (2018) 218.
[4] T.H. Liou, M.H Lin, Characterization of graphene oxide supported porous silica for effectively enhancing adsorption of dyes, Sep. Sci. Technol., 55 (2020) 431–443.
[5] G.M. Ratnamala, U.B. Deshannavar, S. Munyal, K. Tashildar, S. Patil, A. Shinde, Adsorption of reactive blue dye from aqueous solutions using sawdust as adsorbent: optimization, kinetic, and equilibrium studies, Arabian J. Sci. Eng., 41 (2016) 333–344.
[6] J. Mo, Q. Yang, N. Zhang, W. Zhang, Y. Zheng, Z. Zhang, A review on agro-industrial waste (AIW) derived adsorbents for water and wastewater treatment, J. Environ. Manage., 227 (2018) 395–405.
[7] L. Zhou, H. Zhou, Y. Hu, S. Yan, J. Yang, Adsorption removal of cationic dyes from aqueous solutions using ceramic adsorbents prepared from industrial waste coal gangue, J. Environ. Manage., 234 (2019) 245–252.
[8] L.B.L. Lim, N. Priyantha, C.M. Chan, D. Matassan, H.I. Chieng, M.R.R. Kooh, Investigation of the sorption characteristics of water lettuce (WL) as a potential low-cost biosorbent for the removal of methyl violet 2B, Desal. Water Treat., 57 (2016) 8319–8329.
[9] L. Zhu, P. Zhu, L. You, S. Li, Bamboo shoot skin: turning waste to a valuable adsorbent for the removal of cationic dye from aqueous solution, Clean Technol. Environ. Policy, 21 (2019) 81–92.
[10] S.S. Iman, H.F. Babamale, A short review on the removal of Rhodamine B dye using agricultural waste-based adsorbents, Asian J. Chem. Sci., 7 (2020) 25–37.
[11] R. Rehman, S. Farooq, T. Mahmud, Use of agro-waste *Musa acuminata* and *Solanum tuberosum* peels for economical sorptive removal of emerald green dye in ecofriendly way, J. Cleaner Prod., 206 (2019) 819–826.
[12] L.B.L. Lim, N. Priyantha, H.I. Chieng, M.K. Dahri, *Artocarpus camansi* Blanco (Breadnut) core as low-cost adsorbent for the removal of methylene blue: equilibrium, thermodynamics, and kinetics studies, Desal. Water Treat., 57 (2016) 5673–5685.
[13] A. Bhatnagar, A.K. Minocha, Assessment of the biosorption characteristics of lychee (*Litchi chinensis*) peel waste for the removal of acid blue 25 dye from water, Environ. Technol., 31 (2010) 97–105.
[14] M.K. Dahri, H.I. Chieng, L.B.L. Lim, N. Priyantha, C.C. Mei, Cempedak durian (*Artocarpus* sp.) peel as a biosorbent for the removal of toxic methyl violet 2B from aqueous solution, Korean Chem. Eng. Res., 53 (2015) 576–583.
[15] F. Temesgen, N. Gabbiye, O. Sahu, Biosorption of reactive red dye (RRD) on activated surface of banana and orange peels: economical alternative for textile effluent, Surf. Interfaces, 12 (2018) 151–159.
[16] L.B.L. Lim, N. Priyantha, C. Hei Ing, M. Khairud Dahri, D.T.B. Tennakoon, T. Zehra, M. Suklueng, *Artocarpus odoratissimus* skin as a potential low-cost biosorbent for the removal of methylene blue and methyl violet 2B, Desal. Water Treat., 53 (2015) 964–975.
[17] A.H. Jawad, R. Razuan, J.N. Appaturi, L.D. Wilson, Adsorption and mechanism study for methylene blue dye removal with carbonized watermelon (*Citrullus lanatus*) rind prepared via one-step liquid phase H^2SO^4 activation, Surf. Interfaces, 16 (2019) 76–84.
[18] H.I. Chieng, L.B.L. Lim, N. Priyantha, D.T.B. Tennakoon, Sorption characteristics of peat of Brunei Darussalam III: equilibrium and kinetics studies on adsorption of crystal violet (CV), Int. J. Earth Sci. Eng., 6 (2013) 791–801.
[19] L. Bulgariu, L.B. Escudero, O.S. Bello, M. Iqbal, J. Nisar, K.A. Adegoke, F. Alakhras, M. Kornaros, I. Anastopoulos, The utilization of leaf-based adsorbents for dyes removal: a review, J. Mol. Liq., 276 (2019) 728–747.
[20] S. Vahdati-Khajeh, M. Zirak, R.Z. Tejrag, A. Fathi, K. Lamei, B. Eftekhari-Sis, Biocompatible magnetic N-rich activated carbon from egg white biomass and sucrose: preparation, characterization and investigation of dye adsorption capacity from aqueous solution, Surf. Interfaces, 15 (2019) 157–165.
[21] L. Zhang, L. Sellaoui, D. Franco, G.L. Dotto, A. Bajahzar, H. Belmabrouk, A. Bonilla-Petriciolet, M.L.S. Oliveira, Z. Li, Adsorption of dyes brilliant blue, sunset yellow and tartrazine from aqueous solution on chitosan: analytical interpretation via multilayer statistical physics model, Chem. Eng. J., 382 (2020) 122952.
[22] Y. Zhou, J. Lu, Y. Zhou, Y. Liu, Recent advances for dyes removal using novel adsorbents: a review, Environ. Pollut., 252 (2019) 352–365.
[23] Z. Li, L. Sellaoui, D. Franco, M.S. Netto, Q. Li, Adsorption of hazardous dyes on functionlized multiwalled carbon nanotubes in single and binary systems: experimental study and physicochemical interpretation of the adsorption mechanism, Chem. Eng. J., 3891 (2020) 124467.
[24] Z.M. Hussin, N. Talib, N.M. Hussin, M.A.K.M. Hanafiah, W.K.A.W.M. Khalir, methylene blue adsorption onto NaOH modified durian leaf powder: isotherm and kinetic studies, Am. J. Environ. Eng., 5 (2015) 38–43.
[25] M. Goswami, P. Phukan, Enhanced adsorption of cationic dyes using sulfonic acid modified activated carbon, J. Environ. Chem. Eng., 5 (2017) 3508–3517.
[26] H.I. Chieng, L.B.L. Lim, N. Priyantha, Enhancing adsorption capacity of toxic malachite green dye through chemically modified breadnut peel: equilibrium, thermodynamics, kinetics and regeneration studies, Environ. Technol., 36 (2015) 86–97.
[27] J. Chen, S. Liu, H. Ge, Y. Zou, A hydrophobic bio-adsorbent synthesized by nanoparticle-modified graphene oxide coated corn straw pith for dye adsorption and photocatalytic degradation, Environ. Technol., (2019) 1–13, doi: 10.1080/09593330.2019.1616827
[28] V. Kumar, V. Rehani, B.S. Kaith, S. Saruchi, Synthesis of a biodegradable interpenetrating polymer network of Av-cl-poly(AA-ipn-AAm) for malachite green dye removal: kinetics and thermodynamic studies, RSC Adv., 8 (2018) 41920–41937.
[29] E.A. Moawed, A.E. Wahba, R.A. Gabr, Synthesis and application of LGB/St/Al_2O_3 biocomposite for sensitive detection and efficient removal of brilliant green dye from wastewater, J. Environ. Chem. Eng., 6 (2018) 7225–7232.
[30] W.S. Wan Ngah, M.A.K.M. Hanafiah, Removal of heavy metal ions from wastewater by chemically modified plant wastes as adsorbents: a review, Bioresour. Technol., 99 (2008) 3935–3948.
[31] M.K. Dahri, M.R.R. Kooh, L.B.L. Lim, Artificial neural network approach for modelling of methyl violet 2B dye adsorption using pomelo skin, J. Environ. Biotechnol. Res., 6 (2017) 238–247.
[32] M.K. Dahri, M.R.R. Kooh, L.B.L. Lim, Adsorption characteristics of pomelo skin toward toxic brilliant green dye, Sci. Bruneiana, 16 (2017) 49–56.

[33] M. Jayarajan, R. Arunachala, G. Annadurai, Use of low cost nano-porous materials of pomelo fruit peel wastes in removal of textile dye, Res. J. Environ. Sci., 5 (2011) 434–443.
[34] L.B.L. Lim, N. Priyantha, Y. Lu, N.A.H.M. Zaidi, Effective removal of methyl violet dye using pomelo leaves as a new low-cost adsorbent, Desal. Water Treat., 110 (2018) 264–274.
[35] L.B.L. Lim, N. Priyantha, Y. Lu, N.A.H. Mohamad Zaidi, Adsorption of heavy metal lead using *Citrus grandis* (Pomelo) leaves as low-cost adsorbent, Desal. Water Treat., 166 (2019) 44–52.
[36] L.B.L. Lim, N. Priyantha, K.J. Mek, N.A.H.M. Zaidi, Application of *Momordica charantia* (bitter gourd) waste for the removal of malachite green dye from aqueous solution, Desal. Water Treat., 154 (2019) 385–394.
[37] L.B.L. Lim, N. Priyantha, N.H. Mohd Mansor, Utilizing *Artocarpus altilis* (breadfruit) skin for the removal of malachite green: isotherm, kinetics, regeneration, and column studies, Desal. Water Treat., 57 (2016) 16601–16610.
[38] C.G. Boeriu, D. Bravo, R.J.A. Gosselink, J.E.G. van Dam, Characterisation of structure-dependent functional properties of lignin with infrared spectroscopy, Ind. Crops Prod., 20 (2004) 205–218.
[39] S. Lagergren, About the theory of so-called adsorption of soluble substances, K. Sven. Vetensk. Akad. Handl., 24 (1898) 1–39.
[40] Y.S. Ho, G. McKay, Sorption of dye from aqueous solution by peat, Chem. Eng. J., 70 (1998) 115–124.
[41] X. Wang, Y. Guo, X. Nan, S. Shi, X. Wang, X. Zhang, Preparation of inverse opal adsorbent by water-soluble colloidal crystal template to obtain ultrahigh adsorption capacity for salicylic acid removal from aqueous solution, J. Hazard. Mater., 371 (2019) 362–369.
[42] W. Weber, J. Morris, Kinetics of adsorption on carbon from solution, J. Sanitary Eng. Div., 89 (1963) 31–60.
[43] W.H. Cheung, Y.S. Szeto, G. McKay, Intraparticle diffusion processes during acid dye adsorption onto chitosan, Bioresour. Technol., 98 (2007) 2897–2904.
[44] I. Langmuir, The adsorption of gases on plane surfaces of glass, mica and platinum, J. Am. Chem. Soc., 40 (1918) 1361–1403.
[45] H. Freundlich, Over the adsorption in the solution, J. Phys. Chem., 57 (1906) 385–470.
[46] V. Pyzhev, M.J. Temkin, Kinetics of ammonia synthesis on promoted iron catalysts, Acta Physiochim., 12 (1940) 217.
[47] D.L. Peterson, O. Redlich, A useful adsorption isotherm, J. Phys. Chem., 63 (1959) 1024–1024.
[48] R. Sips, On the structure of a catalyst surface, J. Chem. Phys., 16 (1948) 490–495.
[49] R.R. Krishni, K.Y. Foo, B.H. Hameed, Adsorption of methylene blue onto papaya leaves: comparison of linear and nonlinear isotherm analysis, Desal. Water Treat., 52 (2014) 6712–6719.
[50] M.L. Mathew, A. Gopalakrishnan, C.T. Aravindakumar, U.K. Aravind, Low-cost multilayered green fiber for the treatment of textile industry waste water, J. Hazard. Mater., 3655 (2019) 297–305.
[51] N.D. Tissera, R.N. Wijesena, H. Yasasri, K.M.N. de Silva, R.M. de Silva, Fibrous keratin protein bio micro structure for efficient removal of hazardous dye waste from water: surface charge mediated interfaces for multiple adsorption desorption cycles, Mater. Chem. Phys., 2461 (2020) 122790.
[52] S.K. Brar, N. Wangoo, R.K. Sharma, Enhanced and selective adsorption of cationic dyes using novel biocompatible self-assembled peptide fibrils, J. Environ. Manage., 2551 (2020) 109804.
[53] H.V. Mehr, J. Saffari, S.Z. Mohammadi, S. Shojaei, The removal of methyl violet 2B dye using palm kernel activated carbon: thermodynamic and kinetics model, Int. J. Environ. Sci. Technol., 17 (2020) 1773–1782.
[54] K. Saeed, M. Ishaq, S. Sultan, I. Ahmad, Removal of methyl violet 2B from aqueous solutions using untreated and magnetite-impregnated almond shell as adsorbents, Desal. Water Treat., 57 (2016) 13484–13493.
[55] K. Samal, N. Raj, K. Mohanty, Saponin extracted waste biomass of *Sapindus mukorossi* for adsorption of methyl violet dye in aqueous system, Surf. Interfaces, 4 (2019) 166–174.
[56] B. Bano, E. Zahir, Comparative study of raw and chemically treated mangrove leaf for remediation of 304 methyl violet 2B dye from aqueous solution: thermo-kinetics aspect, Water Sci. Technol., 73 (2016) 1301–1312.
[57] A. Guzmán-Vargas, E. Lima, G.A. Uriostegui-Ortega, M.A. Oliver-Tolentino, E.E. Rodríguez, Adsorption and subsequent partial photodegradation of methyl violet 2B on Cu/Al layered double hydroxides, Appl. Surf. Sci., 363 (2016) 372–380.
[58] L.R. Bonetto, F. Ferrarini, C. de Marco, J.S. Crespo, R. Guégan, M. Giovanela, Removal of methyl violet 2B dye from aqueous solution using a magnetic composite as an adsorbent, J. Water Process Eng., 6 (2015) 11–20.
[59] L.B.L. Lim, N. Priyantha, N.A.H. Mohamad Zaidi, A superb modified new adsorbent, *Artocarpus odoratissimus* leaves, for removal of cationic methyl violet 2B dye, Environ. Earth Sci., 75 (2016) 1179, doi: 10.1007/s12665-016-5969-7.
[60] Y. Tang, Q. Zhou, Y. Zhao, Y. Peng, Efficient removal of methyl violet from aqueous solution by a low-cost adsorbent camphora fallen leaves powder, J. Dispersion Sci. Technol., 38 (2017) 1135–1141.
[61] Y. Tang, Y. Li, Y. Zhao, Q. Zhou, Y. Peng, Enhanced removal of methyl violet using NaOH-modified camphora leaves powder and its renewable adsorption, Desal. Water Treat., 98 (2017) 306–314.
[62] S.S. Behera, S. Das, B.M. Murmu, R.K. Mohapatra, T.R. Sahoo, P.K. Parhi, Kinetics, thermodynamics and isotherm studies on adsorption of methyl violet from aqueous solution using activated bio-adsorbent: *Phragmites* karka, Curr. Environ. Eng., 3 (2016) 229–241.
[63] Y. Kim, J. Bae, H. Park, J.K. Suh, Y.W. You, H. Choi, Adsorption dynamics of methyl violet onto granulated mesoporous carbon: facile synthesis and adsorption kinetics, Water Res., 101 (2016) 187–194.
[64] H. Ying, G. He, L. Zhang, Q. Lei, Y. Guo, W. Fang, Hyperbranched polyglycerol/poly(acrylic acid) hydrogel for the efficient removal of methyl violet from aqueous solutions, J. Appl. Polym. Sci., 133 (2016) 42951, doi: 10.1002/app.42951.
[65] L.B.L. Lim, N. Priyantha, C.M. Chan, D. Matassan, H.I. Chieng, M.R.R. Kooh, Adsorption behavior of methyl violet 2B using duckweed: equilibrium and kinetics studies, Arabian J. Sci. Eng., 39 (2014) 6757–6765.
[66] M.I. Din, K. Ijaz, K. Naseem, Biosorption potentials of acid modified Saccharum bengalense for removal of methyl violet from aqueous solutions, Chem. Ind. Chem. Eng. Q., 23 (2017) 399–409.
[67] R. Foroutan, R. Mohammadi, S. Farjadfard, H. Esmaeili, B. Ramavandi, G.A. Sorial, Eggshell nano-particle potential for methyl violet and mercury ion removal: surface study and field application, Adv. Powder Technol., 30 (2019) 2188–2199.
[68] S.M. Musyoka, H. Mittal, S.B. Mishra, J.C. Ngila, Effect of functionalization on the adsorption capacity of cellulose for the removal of methyl violet, Int. J. Biol. Macromol., 65 (2014) 389–397.
[69] M.R.R. Kooh, M.K. Dahri, L.B.L. Lim, Removal of the methyl violet 2B dye from aqueous solution using sustainable adsorbent *Artocarpus odoratissimus* stem axis, Appl. Water Sci., 7 (2017) 3573–3581.
[70] L.B.L. Lim, N. Priyantha, X.H. Bong, N.A.H.M. Zaidi, Enhancement of adsorption characteristics of Methyl violet 2B dye through NaOH treatment of *Cucumis melo var. cantalupensis* (rock melon) skin, Desal. Water Treat., 180 (2020) 336–348.
[71] C. Li, Y. Dong, J. Yang, Y. Li, C. Huang, Modified nano-graphite/Fe_3O_4 composite as efficient adsorbent for the removal of methyl violet from aqueous solution, J. Mol. Liq., 196 (2014) 348–356.
[72] X. Song, Y. Wang, K. Wang, R. Xu, Low-Cost carbon nanospheres for efficient removal of organic dyes from aqueous solutions, Ind. Eng. Chem. Res., 51 (2012) 13438–13444.
[73] Y. Wang, Y. Xie, Y. Zhang, S. Tang, C. Guo, J. Wu, R. Lau, Anionic and cationic dyes adsorption on porous poly-melamine-formaldehyde polymer, Chem. Eng. Res. Des., 114 (2016) 258–267.
[74] A.J. Miola, M.A. Campagnolo, D.C. Dragunski, D. Schwantes, E.A.V. Leismann, G.F. Coelho, A.C. Gonçalves, C.R.T. Tarley,

Chemical modifications of cassava peel as adsorbent material for metals ions from wastewater, J. Chem., 2016 (2016) 1–15.
[75] N.A.H.M. Zaidi, L.B.L. Lim, A. Usman, Enhancing adsorption of malachite green dye using base-modified *Artocarpus odoratissimus* leaves as adsorbents, Environ. Technol. Innovation, 13 (2019) 211–223.
[76] E. Daneshvar, A. Vazirzadeh, A. Niazi, M. Kousha, M. Naushad, A. Bhatnagar, Desorption of Methylene blue dye from brown macroalga: effects of operating parameters, isotherm study and kinetic modeling, J. Cleaner Prod., 152 (2017) 443–453.
[77] S. Chowdhury, R. Mishra, P. Saha, P. Kushwaha, Adsorption thermodynamics, kinetics and isosteric heat of adsorption of malachite green onto chemically modified rice husk, Desalination, 265 (2011) 159–168.
[78] M.K. Dahri, M.R.R. Kooh, L.B.L. Lim, Water remediation using low cost adsorbent walnut shell for removal of malachite green: equilibrium, kinetics, thermodynamic and regeneration studies, J. Environ. Chem. Eng., 2 (2014) 1434–1444.
[79] L.B.L. Lim, N. Priyantha, K.J. Mek, N.A.H.M. Zaidi, Potential use of *Momordica charantia* (bitter gourd) waste as a low-cost adsorbent to remove toxic crystal violet dye, Desal. Water Treat., 82 (2017) 121–130.